Наносистеми, наноматеріали, нанотехнології
Nanosistemi, Nanomateriali, Nanotehnologii
2024, т. 22, № 3, сс. 557–568
https://doi.org/10.15407/nnn.22.03.557

PACS numbers: 68.37.Hk, 68.37.Lp, 68.37.Vj, 78.67.Bf, 81.16.Mk, 87.19.xb, 87.64.Cc

Synthesis of Silver Nanoparticles *via* Pulsed-Laser Ablation in Deionized Water: Characterization and Antibacterial Applications

Khalaf Ajaj[1], Mushtaq Abed Al-Jubbori[2], and Abdullah M. Ali[1]

[1]*College of Education for Pure Sciences,*
Department of Physics,
University of Tikrit,
41001 Mosul, Iraq
[2]*College of Education for Pure Sciences,*
Department of Physics,
University of Mosul,
41001 Mosul, Iraq

In this present study, the fabrication of silver nanoparticles (NPs) is achieved through *Q*-switched Nd:YAG-laser ablation. A disc-shaped silver target immersed in deionized water served as the substrate for the ablation process. Varying number of pulses, specifically, 300 and 500 pulses, is used along with two laser fluences of 6.36 J/cm^2 and 12.73 J/cm^2. To ascertain the nanoparticles' morphological and optical attributes, UV–Vis spectrophotometry, transmission electron microscopy (TEM) and field-emission scanning electron microscopy (FE-SEM) analyses are employed. The augmentation of absorbance spectra proportional to pulse counts indicates escalated silver-nanoparticles' concentrations. The absorption spectra exhibit surface-plasmon resonance peaks at ≅ 400 nm, which are intensified with increasing laser pulses. An observable decrease in the optical band gap is also noted. TEM and FE-SEM analyses corroborate the existence of nearly spherical Ag nanoparticles. The analyses reveal their average diameters of approximately 34 nm and 57 nm for laser fluences of 6.36 J/cm^2 and 12.73 J/cm^2, respectively. Intriguingly, the inhibitory effect on *Klebsiella pneumoniae* and *Staphylococcus aureus* is more pronounced with Ag NPs generated at lower laser fluence, despite the equivalent pulse number.

У цьому дослідженні виготовлення наночастинок (НЧ) срібла було досягнуто за допомогою абляції лазером Nd:YAG із модуляцією добротности. Срібна мішень у формі диска, занурена у дейонізовану воду, слугувала підкладинкою у процесі абляції. Було застосовано різну кіль-

кість імпульсів, а саме, 300 і 500 імпульсів, разом із двома лазерними флюєнсами у 6,36 Дж/см^2 і 12,73 Дж/см^2. Щоб визначити морфологічні й оптичні характеристики наночастинок, використовували спектрофотометрію УФ- і видимого діяпазонів, трансмісійну електронну мікроскопію (ТЕМ) і сканувальну електронну мікроскопію за допомогою польової емісії (ПМ-СЕМ). Збільшення спектрів вбирання пропорційно кількості імпульсів вказувало на підвищення концентрації наночастинок срібла. Спектри вбирання показали піки поверхневого плазмонного резонансу в околі ≅ 400 нм, які посилювалися зі збільшенням лазерних імпульсів. Також було відзначено помітне зменшення ширини забороненої зони. Аналіза даних ТЕМ і ПЕ-СЕМ підтвердила наявність майже сферичних наночастинок срібла. Аналіза виявила їхні середні діяметри приблизно у 34 нм і 57 нм для потоків лазерного світла у 6,36 Дж/см^2 і 12,73 Дж/см^2 відповідно. Цікаво, що інгібувальна дія на *Klebsiella pneumoniae* та *Staphylococcus aureus* була більш вираженою з Ag НЧ, створеними за меншого потоку лазерного світла, незважаючи на еквівалентну кількість імпульсів.

Key words: laser ablation, silver nanoparticles, nanoparticle size, antibacterial activity.

Ключові слова: лазерна абляція, наночастинки срібла, розмір наночастинок, антибактеріяльна активність.

(Received 17 August, 2023)

1. INTRODUCTION

In the past ten years or so, there has been a significant increase in the risk of biological and bacterial attacks, particularly, in areas, which are used for human consumption, like food, food packaging and water. Scientists have been inspired by the rising risk to create new, risk-free, and simple-to-use inorganic antibacterial nanoparticle substances. Certain materials, like metal-oxide semi-conductors, could produce entirely new materials with optical and/or electronic properties, when their dimensions are shrunk to the nanoscale. This makes it possible for researchers to examine the advantages of nanomaterials in a variety of fields, including biomedicine, optoelectronics and the environment [1–3].

The use of nanoparticles as new agents to inhibit microbial growth has increased as a result of the development of antibiotic resistance [4]. Optimized synthesis of nanoparticles (NPs) increased the production of ultrapure and perfectly spherical NPs with smaller average sizes [5]. Ultrashort laser-pulse interaction with materials has received much attention from researchers in micro and nanomachining, especially for the generation of nanoparticles in liquid environments, because of the straightforward method and direct

application for organic solvents. In addition, the colloidal nanoparticles produced by laser ablation have very high purity they are free from surfactants and reaction products [6]. Moreover, the pulsed-laser ablation in liquid (PLAL) technique is gaining more importance due to its simplicity, rapid rate of formation of nanoparticles and eco-friendly approach [7]. There are numerous literature papers on laser interaction with hard and soft materials that focus on potential future applications in the fields of biomedicine and nanoenergy production [8]. Typical laser parameters that affect the ablation rate include wavelength, fluence, pulse duration, repetition rate, the target materials' ability to absorb light, transmission, laser pulse energy, and the chemical makeup of the liquid [9–11].

Laser parameters can be used to modify the size, shape, surface properties, aggregation state, solubility, structure, and chemical makeup of nanoparticles. The same processes could be used with various types of materials to create nanostructured materials in a variety of shapes and sizes. Besides, when a solid target is ablated in liquid, hot plasma is created, the surrounding liquid is vaporized, and a cavitation bubble (CB) is created. In this bubble, target atoms and clusters as well as liquid species can react under extreme pressure and temperature conditions. The ablation products quickly cool to room temperature once they are released into the surrounding liquid [12].

Among all metallic nanoparticles, silver NPs have the most intriguing physical characteristics for biosensing, and its antimicrobial properties can be improved by adjusting its size at the nanoscale. Additionally, Ag NPs with nanoscale sizes demonstrated potent bactericidal activity against both gram-positive and gram-negative bacteria. However, this technique is preferred for producing nanoparticles because it does not involve any potentially dangerous materials. In other techniques, the nanoparticles are contaminated with substances that might be harmful to human cells due to the use of surfactants or chemical precursors [13, 14]. A metallic-nanoparticles' surface-plasmon resonance peak (SPRP) is produced, when light excite the electrons within it, resulting in a resonant oscillation in the visible range, the SPRP is related to the size of the particle [15]. Gram-negative rod-shaped bacilli known as *Klebsiella* bacteria can be found in the intestines of people, animals and the environment [16]. A typical species of *Klebsiella pneumoniae* is known to cause a number of infections in people, including pneumonia, intra-abdominal infections, and urinary tract infections. Additionally, it is a pathogen, which is multidrug resistant and frequently causes serious morbidity and mortality in healthcare settings [17]. Besides that, *Staphylococcus aureus* is a gram-positive coccus that can cause a variety of clinical infections, such as abscesses, pneumonia, sepsis

and it is a significant contributor to food poisoning [18, 19]. *S. aureus* has the capacity to develop resistance to antimicrobial agents, making treatment and control of infections challenging [20].

The current study uses the PLAL technique to create silver nanoparticles under controlling the number of pulses and ablated energies. Using UV–Visible spectrophotometer, transmission electron microscopy and field-emission scanning electron microscopy analyses, the optical and morphology characteristics of the prepared samples were examined. Ag NPs were used to test the antibacterial effectiveness against *Klebsiella pneumoniae* and *Staphylococcus aureus*.

2. EXPERIMENTAL METHODS

2.1. Preparation of Silver Nanoparticles

A silver metal plate (high-purity of 99.99%) disc-shaped with dimensions 2 cm in diameter and 2 mm thick, Ag target were cleaned with acetone for 5 min before ablation in order to remove the oxide layer that was formed due to exposure to air and was placed at the bottom of the beaker is filled with 5 ml of deionized water (DIW). The distance between the target and the laser source is of 10 cm. Under mechanical stirring, the target was irradiated with the focused output of fundamental wavelength 1064 nm of nanosecond pulsed *Q*-switched Nd:YAG laser with the pulse repetition rate and pulse duration of the laser were 7 Hz and 10 ns, respectively, with operated at two different laser fluences of 6.36 J/cm^2 and 12.73 J/cm^2, and the number of pulses was 300 and 500 pulses for each energy. The experimental setup for laser ablation is illustrated in Fig. 1.

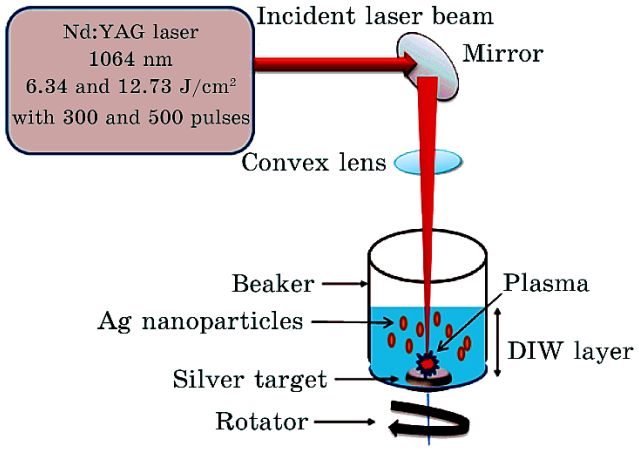

Fig. 1. PLAL system schematic diagram.

2.2. Agar Well Diffusion Method and Antibacterial Activity of Ag NPs

Mueller Hinton agar of 37 g was dissolved in 1 litter of distilled water to form a medium. A sterilization tool known as a syringe (autoclave) was used to sterilize the medium, and the pH was adjusted to 7.2. After that, it is transferred to disposable Petri dishes and put into the refrigerator at 4°C until it is needed. The disposable Petri dishes are placed on a flat surface and poured into them to a depth of about 4 mm. With 500 pulses of samples, the antibacterial activity of laser fluence of 6.36 J/cm^2 and 12.73 J/cm^2 of Ag NPs was assessed against two bacterial strains, *Klebsiella pneumoniae* (gram-negative) and *Staphylococcus aureus* (gram-positive). In this method, the bacteria were thoroughly wiped on the media of the plates using sterile cotton swabs. Then, 150 µl of a solution containing silver NPs was added to the spot that had been prepared for each kind of bacteria. The test organism and Ag NPs were then added to the plates, which were then incubated at 37°C for 24 hours. By observing the inhibition zone and the surface transformation into a transparent layer after incubation, which indicated the inhibition of bacterial growth, it was possible to determine the effect of Ag NPs on the growth of bacteria.

3. RESULTS AND DISCUSSION

3.1. The Optical Absorption Analysis

The spectroscopic absorption of a synthesized colloidal solution of Ag NPs in deionized water was examined using a Shimadzu (UV-1800) UV–Vis spectrophotometer. As shown in Fig. 2, the observed

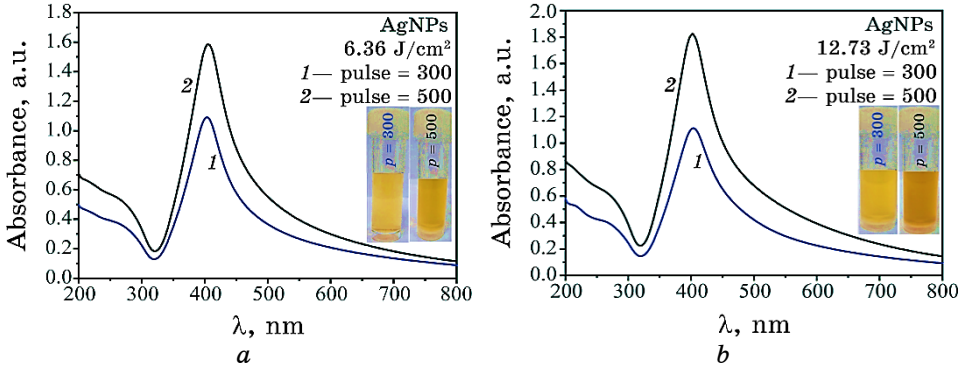

Fig. 2. Absorption spectra of Ag NPs in DIW prepared by PLAL at (*a*) 6.36 J/cm^2 and (*b*) 12.73 J/cm^2 at various numbers of pulses: 300 and 500.

increase in absorption shows that the absorption spectra of silver NPs exhibit absorbance as a function of wavelength. The increase in absorption, as both the number of pulses and the laser fluence increase, indicates an increase in concentration. The colour change of the solution and the appearance of the surface plasmonic resonance peak are considered evidence for the formation of Ag nanoparticles. The elevation has been found to have higher light absorption at ≅ 400 nm, which returns to the SPRP, indicating the formation of spherical particles. Furthermore, on the higher wavelength side, which includes the visible spectrum and wavelengths up to 500 nm, the NPs have a low absorption value (high transmission). It is also shown in the figure that the spectrum of laser fluence is of 12.73 J/cm^2, which is more than 6.36 J/cm^2, that indicates an increase in concentration and possibly size nanoparticles as well.

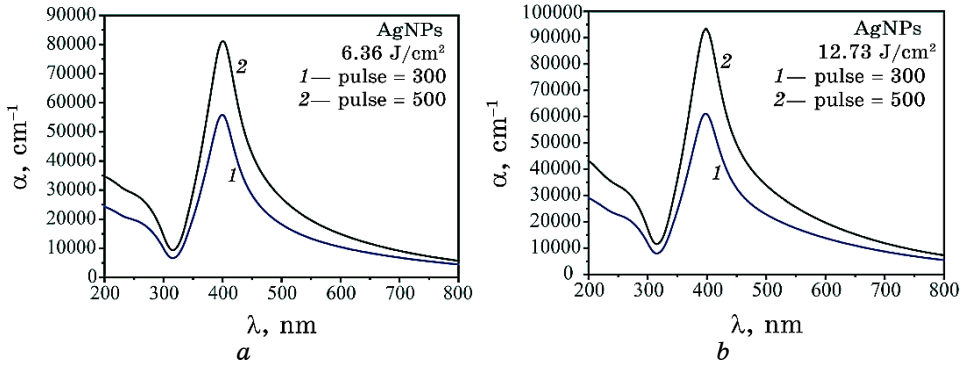

Fig. 3. Absorption coefficient of Ag NPs as a function of wavelength prepared by PLAL at (*a*) 6.36 J/cm^2 and (*b*) 12.73 J/cm^2.

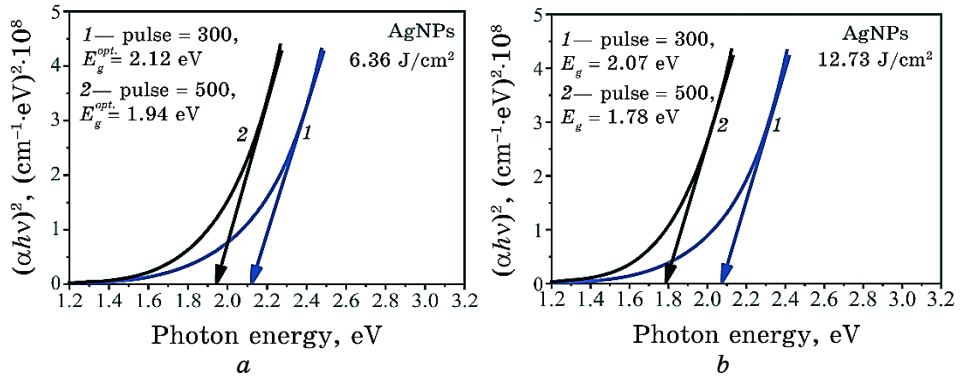

Fig. 4. Optical band gap of the silver NPs prepared at (*a*) 6.36 J/cm^2 and (*b*) 12.73 J/cm^2.

The incident photon energy, as well as the properties of the material itself, has an impact on a materials' absorption coefficient. According to Beer's law, the transmission (T) and reflection (R) spectra are related to the absorption coefficient [21]:

$$\alpha = \frac{1}{d} \log\left[\frac{(1-R)^2}{2T} + \frac{(1-R)^2}{\sqrt{2T^2 + R^2}}\right], \quad (1)$$

where d is the thickness of the sample. The absorption coefficient (α) at the wavelength of maximum absorption increases with the number of pulses and laser fluence, due to the concentration of silver NPs increased as shown in Fig. 3.

An important factor affecting materials' optical and electronic properties is the optical band gap $E_g^{opt.}$ .The optical band gap of the silver NPs was determined using the Tauc plot and UV–Vis spectroscopy. The samples' $E_g^{opt.}$ was calculated by fitting the equation to the data [22]:

$$(\alpha h\nu)^{1/2} = k\left(h\nu - E_g^{opt.}\right), \quad (2)$$

where k is a constant of effective mass, $h\nu$ is the energy of the incident photons.

Figure 4 shows that as the number of pulses increases, the optical band gap experiences a slight decrease. The quantum confinement effect is responsible for this reduction. Additionally, the high laser fluence can also have this effect. The laser fluence can heat up the target more, removing more NPs and making it larger, and the optical energy gap narrowing as a result.

3.2. Particle Size and Morphology Analysis

3.2.1. Transmission Electron Microscopy Analysis

Transmission electron microscopy (TEM) analysis was used to confirm the average particle size and morphology of silver NPs prepared by the PLAL technique at laser fluences of 6.36 J/cm^2 and 12.73 J/cm^2 with 500 pulses.

The TEM image in Fig. 5 shows that NPs have morphology, which is almost spherical. Ag NP diameters are between 37 and 51 nm for 6.36 J/cm^2 and 12.73 J/cm^2. On the other hand, because metal nanoparticles tend to agglomerate, the agglomeration of nanoparticles can be attributed to the absence of antiagglomeration agents in the colloidal aqueous solution.

It is shown by TEM image analysis that, with increasing of laser fluence, the concentration and size of silver nanoparticles increase.

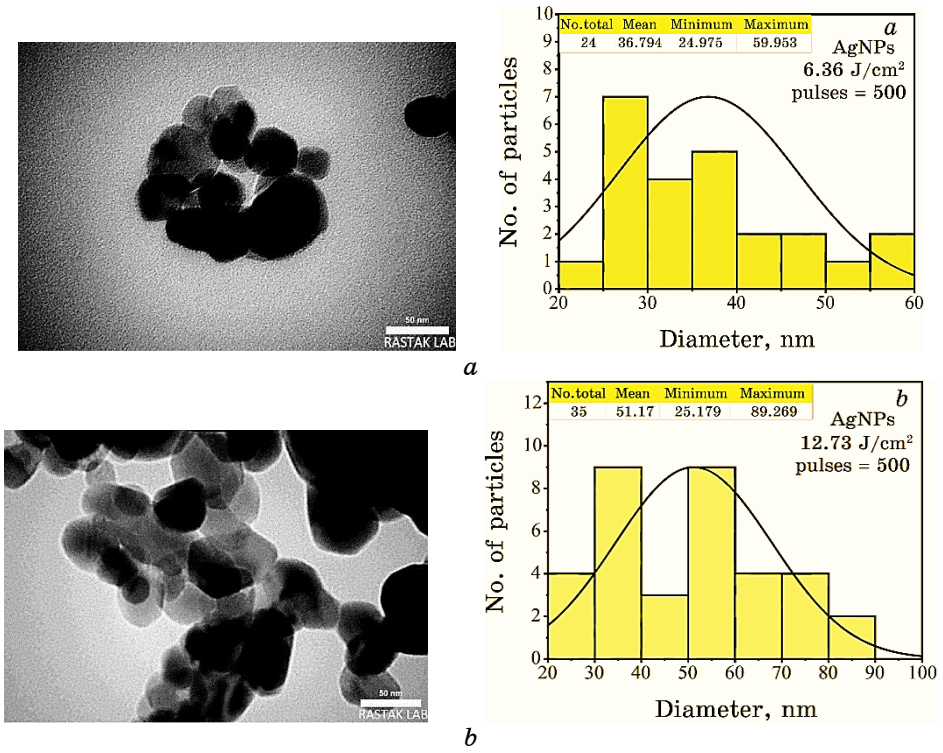

Fig. 5. TEM image of Ag NPs and the particle-size distribution: (*a*) 6.36 J/cm^2, (*b*) 12.73 J/cm^2 at the same number 500 pulses.

3.2.2. Field-Emission Scanning Electron Microscopy Analysis

Utilizing the field-emission scanning electron microscopy (FE-SEM) analysis at a 200 k× magnification, it possible to analyse the morphology and particle-size distribution of Ag NPs at 6.36 J/cm^2 and 12.73 J/cm^2 with 500 pulses. In Figure 6, the FE-SEM image and distribution histograms show information for Ag nanoparticles with a size range from 31 nm to 63 nm. The spherical shape and uniform distribution of the nanoparticles are obvious. UV–Vis and TEM measurements support these findings.

3.2.3. Antibacterial Activity of Ag NPs

The inhibitory activity of silver nanoparticles was examined against two bacterial strains: *Klebsiella pneumoniae* and *Staphylococcus aureus*. Using the etch diffusion method on the surface of the agar to determine the effect of the prepared nanoparticles with two laser

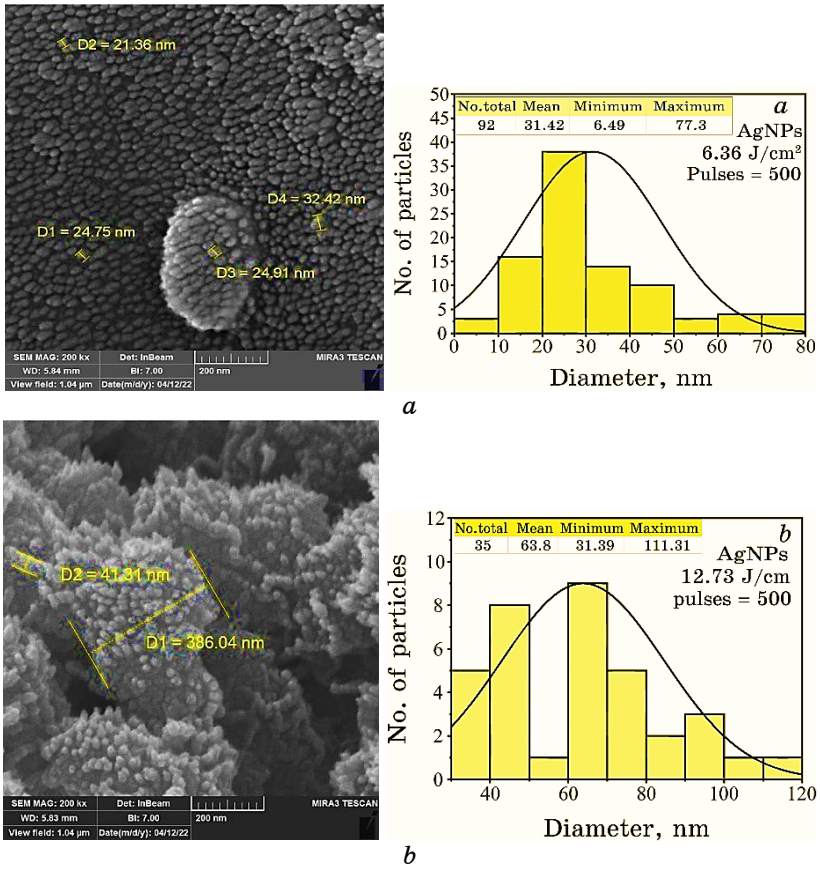

Fig. 6. FE-SEM micrographs of Gaps and the particle size distribution for (*a*) 6.36 J/cm^2 (*b*) 12.73 J/cm^2 at 500 pulses.

fluences of 6.36 J/cm^2 and 12.73 J/cm^2 with 500 pulses. The control medium as a negative control (the solution used in the experiment (DIW)) does not show a growth-inhibiting effect on bacterial strains. Additionally, silver ions released from the nanoparticles can also cause damage to bacterial DNA and interfere with cellular processes. On the other hand, due to particle size, our study reveals that silver NPs exhibit varying degrees of antibacterial activity; it was found through our study that the inhibitory effect of the silver nanoparticles is greater for the particles prepared at 6.36 J/cm^2, more effective compared to the nanoparticles prepared at 12.73 J/cm^2 and with the same number of pulses as shown in Fig. 7 and Fig. 8.

The ability of nanoparticles to interact with cell walls or even pass through them and directly change intracellular components de-

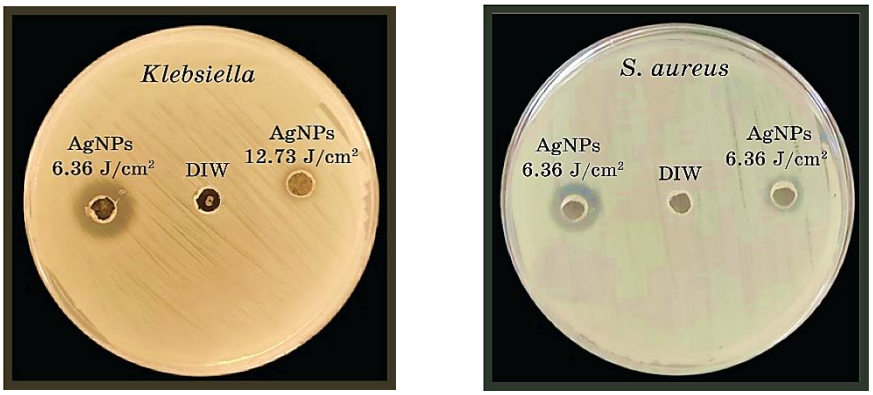

Fig. 7. The antibacterial activity test results for Ag NPs prepared for laser fluences of 6.36 J/cm^2 and 12.73 J/cm^2 at a number of 500 pulses for: (*a*) *Klebsiella* $G(+\upsilon_e)$, (*b*) *S. aureus* $G(-\upsilon_e)$.

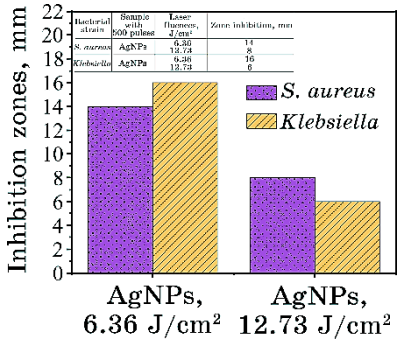

Fig. 8. Histogram for the inhibition zone as a function of the sample prepared for laser fluences of 6.36 J/cm^2 and 12.73 J/cm^2.

pends largely on their physical and chemical properties, such as concentration and type of substance. This also allows them to have an inhibitory effect on pathogenic bacteria. Due to the low concentration of nanoparticles prepared using PLAL technique compared to other techniques, it is observed that there is weak diffusion of NPs, which produces a rather weak inhibition zone.

4. CONCLUSION

Pulsed-laser ablation of a silver target immersed in deionized water is used to synthesize noble metal nanoparticles. The result shows that the ablation rate increased as the number of pulses increased and the

laser fluence increased. The absorption spectra show a sharp and single peak at around 400 nm, which produces a stronger plasmon resonance. TEM and FE-SEM images indicate a change in the size of Ag nanoparticles with increasing laser fluence, and the surface morphology is predominantly spherical. Furthermore, the findings of our study indicate that Ag nanoparticles have an antibacterial effect against both *Klebsiella pneumoniae* and *Staphylococcus aureus*, especially at low laser fluences.

ACKNOWLEDGEMENTS

The authors would like to express their warmest thanks to University of Mosul, College of Education for Pure Science and Department of Physics for supporting this work.

REFERENCES

1. J. S. Golightly and A. W. Castleman, *The Journal of Physical Chemistry B*, **110**, Iss. 40: 19979 (2006); https://doi.org/10.1021/jp062123x
2. K. S. Khashan and M. H. Mohsin, *Surface Review and Letters*, **22**, Iss. 4: 1550055 (2015); https://doi.org/10.1142/S0218625X15500559
3. A. Hamad, K. S. Khashan, and A. Hadi, *Journal of Inorganic and Organometallic Polymers and Materials*, **30**, Iss. 12: 4811 (2020); https://doi.org/10.1007/s10904-020-01744-x
4. R. P. Allaker, *Journal of Dental Research*, **89**, Iss. 11: 1175 (2010); https://doi.org/10.1177/0022034510377794
5. H. Naser, M. A. Alghoul, M. K. Hossain, N. Asim, M. F. Abdullah, M. S. Ali, F. G. Alzubi, and N. Amin, *Journal of Nanoparticle Research*, **21**, Iss. 249: 1 (2019); https://doi.org/10.1007/s11051-019-4690-3
6. S. Stroj, W. Plank, and M. Muendlein, *Applied Physics A*, **127**, Iss. 1: 7 (2021); https://doi.org/10.1007/s00339-020-04192-z
7. S. Z. Mat Isa, R. Zainon, and M. Tamal, *Materials*, **15**, Iss. 3: 875 (2022); https://doi.org/10.3390/ma15030875
8. E. Fazio, A. Scala, S. Grimato, A. Ridolfo, G. Grassi, and F. Neri, *Journal of Materials Chemistry B*, **3**, Iss. 46: 9023 (2015); https://doi.org/10.1039/C5TB01076D
9. D. Riabinina, M. Chaker, and J. Margot, *Nanotechnology*, **23**, Iss. 13: 135603 (2012); https://doi:10.1088/0957-4484/23/13/135603
10. M. Mahdieha and B. Fattahi, *Applied Surface Science*, **329**, Iss. 1: 47 (2015); https://doi.org/10.1016/j.apsusc.2014.12.069
11. G. Guillén, V. Ibarra, I. Palma, B. Krishnan, D. Avellaneda, and S. Shaji, *Chem. Phys. Chem.*, **18**, Iss. 9: 1035 (2017); https://doi.org/10.1002/cphc.201601056
12. J. Long, M. H. Eliceiri, L. Wang, Z. Vangelatos, Y. Ouyang, X. Xie, Y. Zhang, and C. P. Grigoropoulos, *Optics & Laser Technology*, **134**: 106647 (2021); https://doi.org/10.1016/j.optlastec.2020.106647
13. J. S. Kim, E. Kuk, K. N. Yu, J. H. Kim, S. J. Park, H. J. Lee, S. H. Kim,

Y. K. Park, Y. H. Park, C. Y. Hwang, and Y. K. Kim, *Biology and Medicine*, **3**, Iss. 1: 95 (2007); https://doi.org/10.1016/j.nano.2006.12.001
14. J. R. Morones, J. L. Elechiguerra, A. Camacho, K. Holt, J. B. Kouri, J. T. Ramírez, and M. J. Yacaman, *Nanotechnology*, **16**, Iss. 10: 2346 (2005); https://doi.org/10.1088/0957-4484/16/10/059
15. S. Nie and S. R. Emory, *Science*, **275**, Iss. 5303: 1102 (1997); https://doi.org/10.1126/science.275.5303.1102
16. Y. Yibin, C. Yuhua, L. Yongtao, S. Yi, and A. Xiaohui, *Transboundary and Emerging Diseases*, **68**, Iss. 4: 2051 (2021); https://doi.org/10.1111/tbed.13852
17. K. Sathyavathy and B. K. Madhusudhan, *Journal of Pharmaceutical Research International*, **32**, Iss. 21: 12 (2020); https://doi.org/10.9734/jpri/2020/v32i2130745
18. A. Tigabu and A. Getaneh, *Clinical Laboratory*, **67**, Iss. 7: 1539 (2021); https://doi.org/10.7754/Clin.Lab.2020.200930
19. G. A. Nai, D. A. L. Medina, C. A. T. Martelli, M. S. C. de Oliveira, I. D. Caldeira, B. C., Henriques, M. J. S. Portelinha, M. de Carvalho Almeida, L. K. W. Eller, F. V. de Oliveira Neto, and M. E. A. Marques, *Research, Society and Development*, **10**, Iss. 5: e15310514701 (2021); http://dx.doi.org/10.33448/rsd-v10i5.14701
20. M. Miklasińska-Majdanik, *Antibiotics*, **10**, Iss. 11: 1406 (2021); https://doi.org/10.3390/antibiotics10111406
21. I. Saini, J. Rozra, N. Chandak, S. Aggarwal, K. Sharma, and A. Sharma, *Materials Chemistry and Physics*, **139**, Iss. 2–3: 802 (2013); http://dx.doi.org/10.1016/j.matchemphys.2013.02.035
22. J. Tauc, R. Grigorvici, and A. Vancu, *physica status solidi (b)*, **15**, Iss. 2: 627 (1966); https://doi.org/10.1002/pssb.19660150224